Soft Matter

PAPER

View Article Online
View Journal | View Issue

Cite this: *Soft Matter*, 2015, 11, 9379

The effect of nanoclay on the rheology and dynamics of polychlorinated biphenyl†

D. Roy, R. Casalini and C. M. Roland*

Received 17th August 2015,
Accepted 26th September 2015

DOI: 10.1039/c5sm02054a

www.rsc.org/softmatter

The thermal, rheological, and mechanical and dielectric relaxation properties of exfoliated dispersions of montmorillonite clay in a molecular liquid, polychlorobiphenyl (PCB), were studied. The viscosity enhancement at low concentrations of clay ($\lesssim$5%) exceeded by a factor of 50 the increase obtainable with conventional fillers. However, the effect of the nanoclay on the local dynamics, including the glass transition temperature, was quite small. All materials herein conformed to density-scaling of the reorientation relaxation time of the PCB for a common value of the scaling exponent. A new relaxation process was observed in the mixtures, associated with PCB molecules in proximity to the clay surface. This process has an anomalously high dielectric strength, suggesting a means to exploit nanoparticles to achieve large electrical energy absorption. This lower frequency dispersion has a weaker dependence on pressure and density, consistent with dynamics constrained by interactions with the particle surface.

Introduction

In recent years there has been much activity directed to the use of nano-particle fillers, both organic and inorganic, and the application of nano-composites.[1–4] The effect that very small particles have on properties arises from their enormous interfacial area, amplifying interactions (*e.g.*, chemisorption and stress intensification) with the matrix, and from potential geometric effects when the constraints imposed by the particles are commensurate in size with intrinsic length scales of the material. Geometric confinement can accelerate or slow down molecular motions,[5] the contradictory results due in part to the competing effects of constraint mitigation and system-specific attractive interactions between particles and matrix.[6–10]

In this work we studied mixtures of a simple liquid with nanoclay (organically modified silicate), a one-dimensional nano-particle. Nanoclay is relatively easy to disperse and available at low cost, and consequently has been widely investigated, particularly in polymer composites,[11–18] since its discovery in the early '90s.[19] When properly mixed with an appropriate material, the lamellar clay exfoliates into platelets, 1–2 nm thick with lateral dimensions in the range 0.4–1 μm.[20] The propensity for exfoliation arises from substitution of the native sodium cations by ammonia, in order to overcome inter-layer attractions and enhance the silicate's affinity for the host molecules. We blended organically modified montmorillonite with polychlorinated biphenyl (PCB), a highly polar liquid that facilitates dispersion of the clay. PCB's are a mixture of isomers, and thus they do not crystallize, making them good glass-formers. They also have negligible volatility and excellent thermal stability. We measured the rheology and carried out mechanical and dielectric relaxation spectroscopies. From these results, we assess the reinforcement capacity of the particles, as well as their influence on the local dynamics. The clay also gives rise to a new, low-frequency dynamic process. We evaluated the potential to control the orientation of the molecules or manipulate the nanoclay particles by the application of electric or mechanical fields. Finally, in order to investigate PCB composite's density-scaling behavior,[21,22] we determined the equation of state of the liquid.

Experimental

The nanoclay, Cloisite 20 (Southern Clay Products), has a montmorillonite core of layered magnesium, aluminum silicate, surface-reacted with dimethyl, dehydrogenated tallow. The exfoliated platelets have an aspect ratio (breadth to thickness) equal to a few hundred.[23,24] For most experiments the PCB was Aroclor 1262 (62% chlorine by weight), with a few results reported herein for Aroclor 1242 (42% chlorine); these have on average 7 and 3 chlorine atoms per molecule, respectively. Xylene solutions of the organoclay and PCB were prepared, with the former subjected to ultrasound for a few hours to facilitate dispersion, evidenced by a marked increase in viscosity. The solutions were then blended and stirred overnight at 60 °C. Removal of the xylene was achieved in a vacuum oven at 100 °C.

Naval Research Laboratory, Chemistry Division, Code 6120, Washington, DC 20375-5342, USA. E-mail: roland@nrl.navy.mil

† Electronic supplementary information (ESI) available. See DOI: 10.1039/c5sm02054a

Modulated differential scanning calorimetry (MDSC) was carried out with a TA Q100 calorimeter (modulation rate = ±1 K every 40 s). The dynamic mechanical measurements employed an Anton Paar MCR 502 rheometer. The frequency range was $0.001 \leq \omega$ (rad s^{-1}) ≤ 100, at temperatures from −8 to 30 °C. A parallel plate geometry (25 mm diameter) was used, except for strain-dependence measurements, which employed a cone and plate (1° cone angle). Dielectric relaxation spectroscopy was carried out using cylindrical electrodes (15 mm diameter) with a 0.1 mm. PTFE spacer to maintain a constant sample thickness. A Novocontrol Alpha analyzer was used at frequencies from 10^{-3} to 10^{6} Hz. For ambient pressure measurements, the temperature was controlled using a Delta Design model 9023 oven, while the high pressure dielectric measurements used a Manganin pressure vessel and a Tenney Jr. oven. Pressure–volume–temperature (*PVT*) measurements utilized a Gnomix instrument, with the change in specific volume measured during cooling at 0.5 K min^{-1} at pressures from 10 to 200 MPa.

Results

Calorimetry and *PVT*

MDSC measurements were carried out on the neat PCB and the nanocomposites [ESI†]. A small increase in the glass transition temperature was measured at higher concentrations of the clay (Table 1). The heat capacity change at T_g, Δc_p, was reduced by an amount larger than the reduction of PCB content by the added clay. For example, for a volume concentration of clay ϕ = 0.8%, Δc_p was 10% smaller, implying constraints on the PCB; that is, the mobility of PCB molecules in the vicinity of the particles is restricted.

The specific volume, V, of the neat PCB and two nanocomposites was measured as a function of temperature at various pressures; fitting to the Tait equation

$$V(T,P) = \left(a_0 + a_1 T + a_2 T^2\right)\left(1 - 0.894 \ln\left[1 + \frac{P}{b_0 \exp(-b_1 T)}\right]\right) \quad (1)$$

gave the parameters shown in Table 1. The thermal expansion coefficient, α, is lower for the composites than the neat PCB, by an amount larger than the (modest) replacement of the liquid by the clay. This is consistent with the reduction in Δc_p at T_g (Table 1), reflecting local constraints on the PCB from the nano-particles. The change in the compressibility, κ, is almost negligible.

Rheology

Wide angle X-ray scattering from the mixtures showed no diffraction peaks, consistent with exfoliation of the silicate layers.[2,3] The consequently large surface area of the filler is expected to provide significant reinforcement at low concentrations. Fig. 1 shows the dynamic viscosity measured at a low strain amplitude and low rate, as a function of clay content. The marked increase in η is primarily a hydrodynamic effect, due to the negligible deformability of the particles. The behavior can be described by the Guth–Gold equation for rodlike particles[25]

$$\eta(\phi) = \eta_0(1 + 0.67f\phi + 1.62f^2\phi^2) \quad (2)$$

with the parameter f representing the aspect ratio of the particle. Fitting to the viscosity data we obtain $f = 79 \pm 18$. This is smaller than the aspect ratio of an exfoliated clay platelet, which is expected to be on the order of a few hundred. However, f from eqn (2) represents the aspect ratio of an equivalent rod. Since the latter is nm-size in two dimensions, rather than one, this value of f herein is an underestimate. The large reinforcement by the exfoliated clay is evident in the comparison in Fig. 2 to viscosity data for various large (~100 nm diameter) particulate fillers. The viscosity enhancement from the clay is as much as 50-fold greater than that from silica,[26,27] carbon black,[28] or glassy polystyrene particles.[29]

The viscosities in Fig. 1 were measured at low rate (1 rad s^{-1}) and low dynamic strain (~0.1%). The corresponding steady-shear viscosities were about twofold larger; that is, the empirical Cox–Merz rule does not apply. Increase of either the frequency or strain amplitude causes a substantial reduction in both η and the storage modulus, as illustrated in Fig. 3 showing the dependence on strain amplitude of the viscosity of the 2% clay sample. This effect has three possible origins: disruption of a percolated network of the particles (*i.e.*, Payne effect[30]); orientation of the particles; or their strain-induced agglomeration. These effects have been seen previously in polymer nano-composites.[31–33] The Payne effect is associated with a maximum in the loss modulus, reflecting the excess enthalpy associated with interparticle debonding.[30] Since herein there is only a monotonic decrease in the loss, similar to the effect of rate on the viscosity, the Payne effect can be ruled out. Orientation and agglomeration can be distinguished because while the former is spontaneously reversible, the latter is not. Recovery of the viscosity over time was observed (Fig. 3), but the entropic driving force for randomizing the orientation is small, so that the recovery is very slow. However, after simple distributive mixing of the sample, for example by separating the rheometer plates while they are rotating, the viscosity returns to its initial value associated with isotropic arrangement of the particles. Contrarily, recover from agglomeration would require more intense, dispersive mixing at higher stresses.

Table 1 Properties of neat PCB and clay nano-composite (P = 0.1 MPa)

ϕ^a	T_g (K)	Δc_p (J g^{-1} K^{-1})	a_0 (ml g^{-1})	a_1 (ml g^{-1} K^{-1})	a_2 (ml g^{-1} K^{-2})	b_0	b_1	V^b (ml g^{-1})	α^b (K^{-1})	κ^b (MPa^{-1})
0	273.6	0.22	0.617	4.30×10^{-4}	0.7×10^{-7}	283	5.20×10^{-3}	0.617	7.0×10^{-4}	3.6×10^{-4}
0.008	273.5	0.20	0.617	3.39×10^{-4}	4.4×10^{-7}	265	3.03×10^{-3}	0.617	5.8×10^{-4}	3.6×10^{-4}
0.018	274.6	0.19	0.617	3.52×10^{-4}	4.9×10^{-7}	247	2.61×10^{-3}	0.617	5.7×10^{-4}	3.9×10^{-4}

[a] Concentration by volume. [b] At T = 298 K and P = 0.1 MPa.

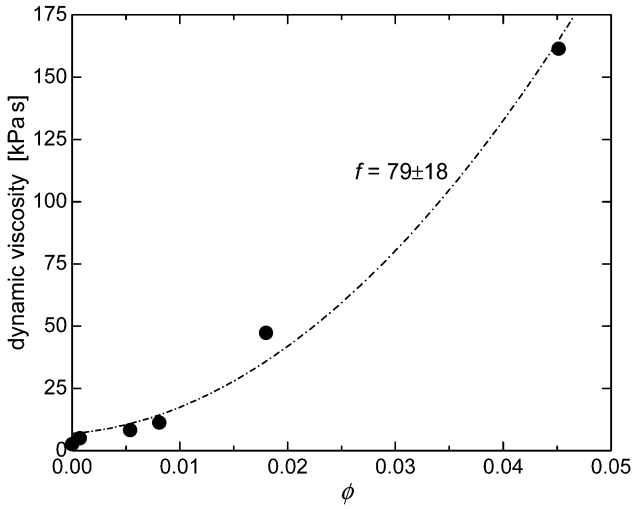

Fig. 1 Dynamic viscosity at 303 K of the PCB62 as a function of the nanoclay volume fraction. The curve through the data is the fitted eqn (2) with the value of the effective shape parameter indicated.

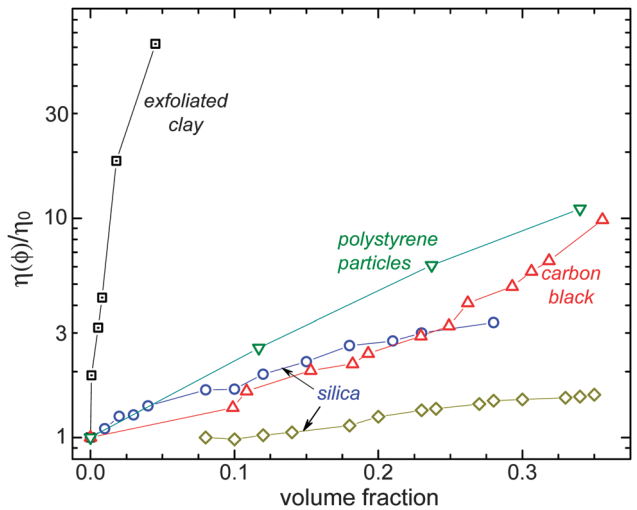

Fig. 2 Viscosity as a function of filler volume fraction, normalized by η for the neat material: nanoclay/PCB62 (squares); polystyrene glassy particles/styrene–butadiene copolymer (inverted triangles[29]); 100 nm silica in polyvinylacetate (circles[26]) and in diisodecyl adipate (diamonds[27]); HAF carbon black/natural rubber (triangles[28]).

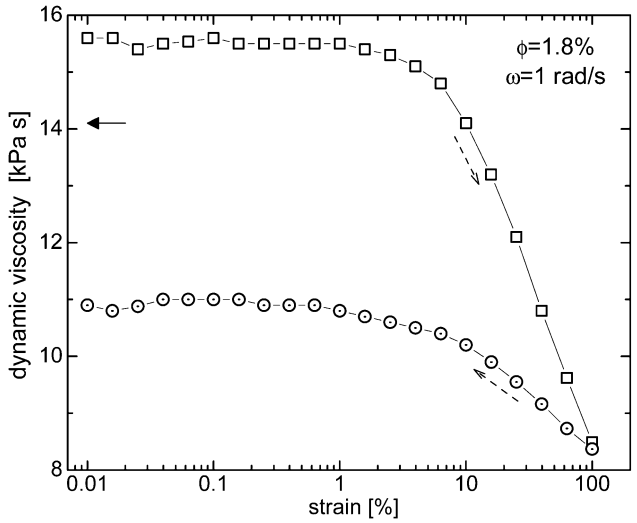

Fig. 3 Variation of viscosity with strain amplitude at 303 K for the nano composite (squares, increasing strain; circles, decreasing strain). As indicated by the arrow, after 4 hours annealing, about 70% of the original magnitude of η is recovered.

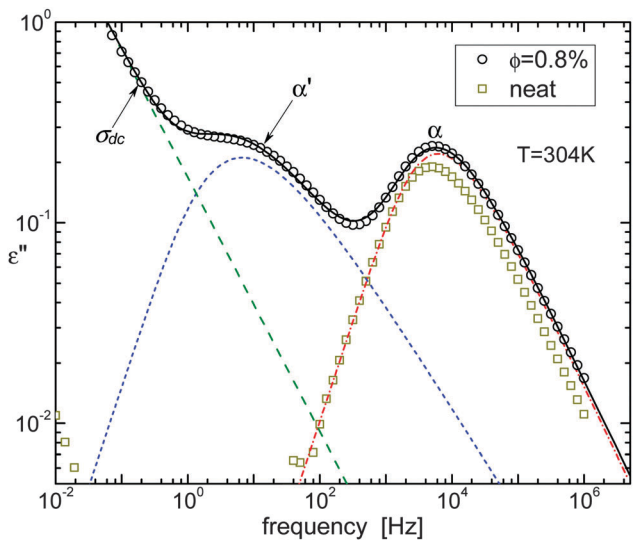

Fig. 4 Dielectric loss spectra of PCB (squares) and nano-composite (circles), along with the fit for the α relaxation (dotted dash line), α′ process (short dashed line), and dc-conductivity contribution (dashed line). The sum of these three contributions is indicated by the solid line. The α peak has been shifted down a bit for clarity.

Local relaxation dynamics

Displayed in Fig. 4 is the dielectric loss measured for the neat PCB62 and ϕ = 0.8%. Both spectra show a prominent α-peak due to molecular reorientation of the polar PCB, but the presence of the clay causes an additional dispersion (α′-process) at lower frequencies. We can describe the two peaks as a superposition of the transform of two Kohlrausch functions[34]

$$\varepsilon^*(f) = \Delta\varepsilon_\alpha L_{i\omega}\left[-\frac{\mathrm{d}\left(\exp\left[-(t/\tau)^\beta\right]\right)}{\mathrm{d}t}\right] \qquad (3)$$

where f is the frequency, τ the relaxation time, $\Delta\varepsilon$ the dielectric strength, β the stretch exponent, and $L_{i\omega}$ indicates the Laplace transform. We simultaneously fit both the real and imaginary part of ε^*, and also included a term for the rise at low frequencies due to dc-conductivity, σ_{dc}

$$\varepsilon''(f) = \frac{\sigma_{\mathrm{dc}}}{\varepsilon_0 2\pi f} \qquad (4)$$

in which ε_0 is the vacuum permittivity. The respective contributions are shown in Fig. 4. There is a negligible difference in the shape of the α peak for the neat PCB and the nano-composite, the stretch exponent varying weakly with temperature, $\beta = 0.67 \pm 0.03$. The α′ peak is somewhat broader, $\beta \sim 0.52 \pm 0.01$.

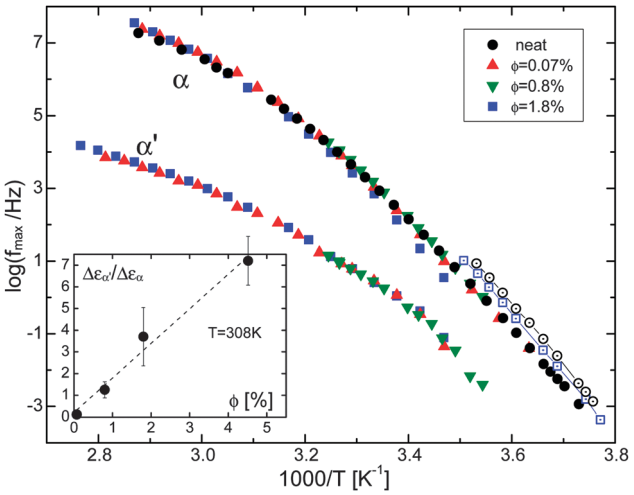

Fig. 5 Arrhenius plots of the frequency of the maximum in the dispersions in the relaxation spectra of neat PCB and four composites having the indicated concentrations by volume of nano-clay. Solid symbols are dielectric measurements and open symbols are dynamic mechanical data. The inset shows the ratio of the dielectric strength for the two processes as a function of clay concentration. The solid line is the linear regression; from the slope we estimate 30 PCB molecules are associated with one formula weight of clay.

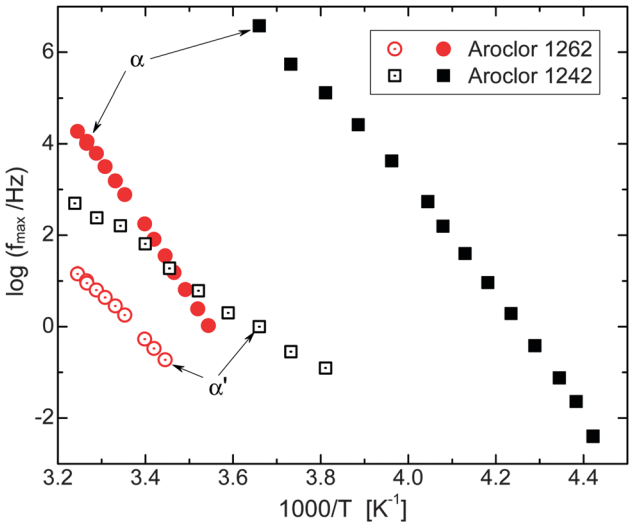

Fig. 6 Comparison of the relaxation frequencies of PCB containing three (squares) and seven (circles) chlorine atoms per molecule. The former has a lower T_g, which shifts the α peak to higher frequencies. However, its larger dipole moment enhances interactions with the clay, and therefore the α′ process is more separated in frequency from the α peak.

The two relaxation times are plotted in Arrhenius form in Fig. 5. There is a weak effect of the clay on the α dynamics, which is barely discernible at lower ϕ. These changes are consistent with the small changes in T_g (Table 1). The α′ peak is 2–3 orders of magnitude lower in frequency than the α dispersion. Interestingly, the α′ peak frequencies are independent of clay concentration. This is inconsistent with an origin due to the build-up of charge at the clay interfaces (*i.e.*, Maxwell–Wagner–Silars polarization[34]). The frequency for such internal polarization varies with the quantity of the conducting component,[35] whereas in Fig. 5 $f_{\alpha'}$ is invariant to composition. The suggestion is that the slower α′ dynamics reflects tethering of the PCB molecules to the clay particles.

The strength of the α′ process depends on the clay concentration; in the inset to Fig. 5 the relative intensity of the α′ and α loss peaks is plotted *versus* clay concentration. The dielectric strengths are anti-correlated, suggesting that the α′ process involves PCB molecules that are interacting with the clay and thus removed from (not participating in) the primary α relaxation. From these data we estimate that ~30 PCB molecules are affected per formula weight of the clay. Assuming no change in dipole moment, this would lead to an α′ intensity that is only *ca.* 10% of that observed. The inference is that the dielectric strength of PCB molecules interacting with the clay is enhanced relative to those remote from the particles. The modified montmorillonite cation has long alkyl chains, which are weakly polar and thus cannot account for the intensity of the α′ process. We speculate that the large $\Delta\varepsilon_{\alpha'}$ is due to cations at the clay surface that are coupled *via* their electrostatic charge to the local PCB motion.

A mixture of the nano-clay with Aroclor 1242, a PCB having 3 chlorine atoms per molecule rather than the 7 for the Aroclor 1262, was also measured. Fewer chlorines results in a higher dipole moment, which should enhance interaction with the clay surface. This is confirmed by measurements of the dielectric relaxation. As seen in Fig. 6, the lower glass transition temperature of Aroclor 1242 shifts the α peak to higher frequencies; however, the α′ process is as much as six decades slower. This indicates the stronger interactions of clay with the more polar PCB causes stronger constraints on the local α′ dynamics.

The mechanical loss modulus was also measured [ESI†]. The α dispersion is somewhat broader than the peak in the dielectric spectra, $\beta \sim 0.63 \pm 0.03$. However for the PCB/clay mixtures, there is no α′ peak; only the primary α process is observed. The implication is that the amplitude of the motion of molecules associated with the clay surface is too small to perturb the local density, whereas their dipole moment is sufficient to give rise to a measurable absorption peak in the dielectric response. The mechanical relaxation frequencies are included in the Arrhenius plot (Fig. 5). Per usual, these are faster than the corresponding dielectric values. (The relationship between dielectric and mechanical dynamics is complex, depending *inter alia* on the respective relaxation strengths.[36]) Similar to the dielectric data, clay reinforcement shifts the mechanical dispersion toward lower frequencies, by about a factor of two.

Effect of volume on the dynamics

The dielectric relaxation times were measured at elevated pressures, with representative results shown in Fig. 7. Both relaxations are slowed by pressure, although the effect is greater for the α process. Since the pressure-dependences are linear, the behavior can be quantified from the activation volume, ΔV, defined as

$$\Delta V = \ln(10) RT \left(\frac{\partial \log \tau}{\partial P}\right)_T \quad (5)$$

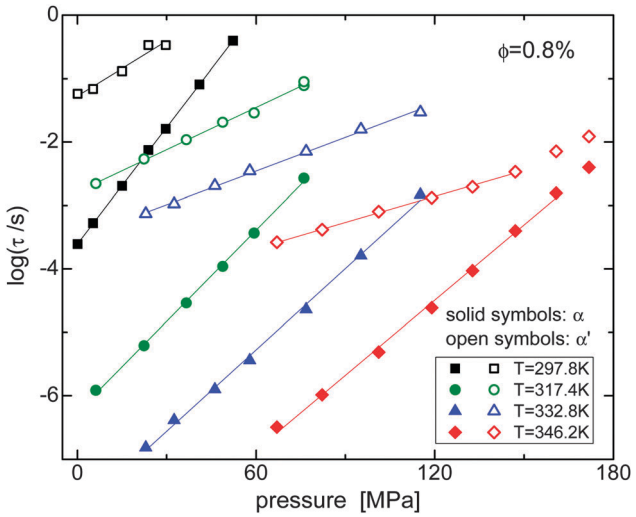

Fig. 7 Relaxation times (defined as the inverse of the peak frequency) for the two processes observed in the nano-composite. The effect of pressure is much weaker for the more local α′ relaxation (open symbols).

where R is the gas constant. These are plotted in Fig. 8 for the data in Fig. 7. The response of the primary process to pressure is the same for the neat PCB and the nano-composite. However, consistent with the more local nature of its motion, the α′ is much less affected by pressure.

For non-associated liquids α relaxation times are uniquely defined by the scaling relationship[21,30]

$$\tau = \Im(TV^{\gamma}) \qquad (6)$$

in which γ is a material-constant and $\Im$ is a generic function, the form of which has been discussed elsewhere.[37] Previously[26] it was found that γ for polyvinylacetate was negligibly affected

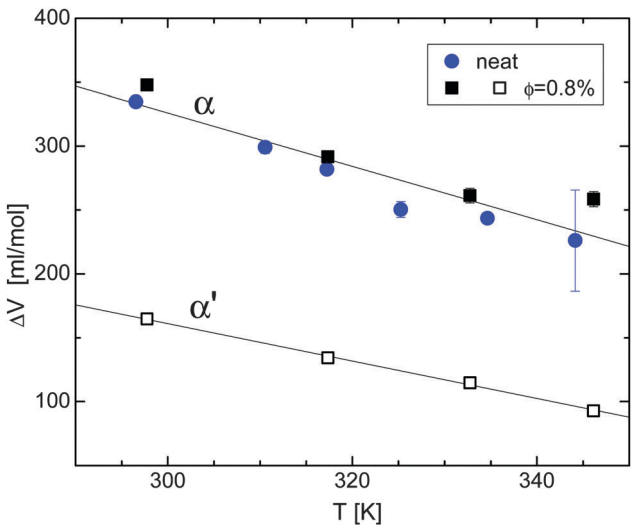

Fig. 8 Activation volumes for the neat PCB (circles) and the nano-composite (squares). The primary relaxation for the two materials is affected equivalently by pressure; however, ΔV is *ca.* twofold smaller for the α′ process and less sensitive to temperature, $-d\Delta V/dT$ = 2.1 and 1.5 for ϕ = 0 and 0.8%, respectively.

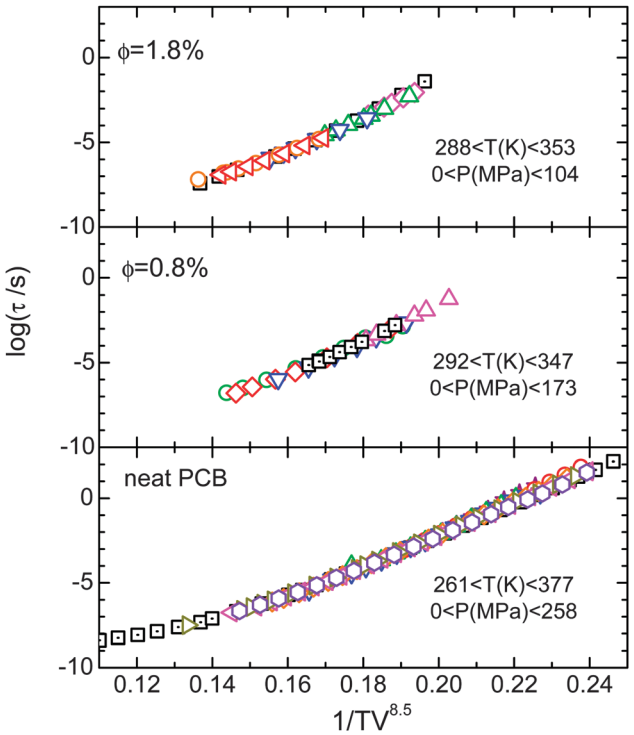

Fig. 9 Density scaling plots of the α relaxation times of PCB, neat and with two concentrations of nanoclay. The scaling exponent, γ = 8.5, is unaffected by the particles. The abscissa is in units of Kelvin and ml g^{-1}. Note that τ for the α′ process superpose (less well) for a smaller value of γ [see ESI†].

by low concentrations of 100 nm silica particles, although at ϕ approaching the percolation threshold there was a significant increase in γ. In Fig. 9 are scaling plots of τ for the α process in neat PCB and two nano-composites; for all three materials, γ = 8.5. This illustrates that at least for clay levels sufficiently low that there is negligible particle–particle interaction, the scaling exponent is unaffected by the particulate reinforcement. This is consistent with the results in Fig. 5 and 8; except for molecules in close proximity to the clay surface, nano-reinforcement has negligible effect on the α relaxation or its pressure dependence.

Applying eqn (6) to the α′ relaxation times, the exponent is much lower, $\gamma \sim 4$, reflecting the weaker pressure dependence of this process. However, the α′ relaxation times superpose poorly *versus* TV^{γ} [ESI†]. This breakdown of the scaling is due to the effect temperature has on the aggregation of the PCB molecules around the clay particles. Scaling behavior arises due to the properties of the intermolecular potential governing dense liquids, in particular its approximation to an inverse power law for interactions relevant to the local dynamics.[38–42] Changes in these interactions due to thermally induced changes in the structure are not accounted for by eqn (6). A similar effect is seen in hydrogen-bonded liquids, which also do not conform to the scaling relation.[43] Notwithstanding the poor scaling, a smaller exponent is consistent with the smaller activation volume for the α′ process. Clearly, motion of molecules near the clay surface is governed by a different potential than that controlling the α relaxation.

Summary

The potential for both new and enhanced properties from nanofillers is well recognized, although the difficulty in dispersing and uniformly distributing such small particles within the host material remains a formidable obstacle to fully exploiting the technology. This dispersion problem is inherent because the defining feature of nanofillers, their enormous specific surface area, necessarily leads to strong interparticle interactions. Thus, the performance benefits from the use of nm particles must be sufficient to warrant the processing issues. Although most work with nanoclay involves polymeric host materials, as seen herein (Fig. 2), the viscosity of the molecular liquid PCB is enhanced fifty times more than can be achieved with conventional fillers, at concentrations (a few percent) well below the percolation threshold. Notwithstanding the effect on the rheology, the structural dynamics (α process), including the response to temperature and pressure, is negligibly affected. However, in the polar matrix used herein, association of molecules in the vicinity of the nanoclay gives rise to a new, anomalously intense dielectric absorption peak. This α′ process, although lower in frequency, comprises more local motions, governed by a different potential than the α relaxation. Such a phenomenon affords a means to design electrical properties that are decoupled from the primary dynamics and the glass transition behavior.

Acknowledgements

This work was supported by the Office of Naval Research. DR acknowledges a National Research Council postdoctoral fellowship. We thank S. Qadri for the WAXS measurements and D. Fragiadakis for enlightening discussions.

References

1 Y. Zhong, Z. Zhu and S. Q. Wang, *Polymer*, 2005, **46**, 3006.
2 Q. T. Ngyuen, D. G. Baird, G. D. Volpe and M. E. Errico, *Adv. Polym. Technol.*, 2006, **25**, 270.
3 M. Avella, S. Cosco, G. D. Volpe and M. E. Errico, *Adv. Polym. Technol.*, 2002, **24**, 132.
4 R. Casalini, R. Bogoslovov, S. B. Qadri and C. M. Roland, *Polymer*, 2012, **53**, 1282–1287.
5 C. M. Roland, *Macromolecules*, 2010, **43**, 7875.
6 C. C. Lin, S. Gam, J. S. Meth, N. Clarke, K. I. Winey and J. Composto, *Macromolecules*, 2013, **46**, 4502.
7 K. Androulaki, K. Chrissopoulou, D. Prevosto, M. Labardi and S. H. Anastasiadis, *ACS Appl. Mater. Interfaces*, 2015, **7**, 12387.
8 H. W. Spiess, *Macromolecules*, 2010, **43**, 5479.
9 Y. H. Lee, A. J. Bur, S. C. Roth and P. R. Start, *Macromolecules*, 2005, **38**, 3828.
10 R. Casalini, D. Prevosto, M. Labardi and C. M. Roland, *ACS Macro Lett.*, 2015, **4**, 1022.
11 R. A. Vaia, H. Ishii and E. P. Giannelis, *Chem. Mater.*, 1993, **5**, 1694.
12 S. S. Ray and M. Okamoto, *Prog. Polym. Sci.*, 2003, **28**, 1539.
13 E. P. Giannelis, R. Krishnamoorti and E. Manias, *Adv. Polym. Sci.*, 1999, **138**, 107.
14 J. Park and S. C. Jana, *Macromolecules*, 2003, **36**, 8391.
15 J. Ma, S. Zhang and Z. Qi, *J. Appl. Polym. Sci.*, 2001, **82**, 1444.
16 Y. Mansoori, K. Roojaei, M. R. Zamanloo and G. Imanzadeh, *Bull. Mater. Sci.*, 2012, **35**, 1063.
17 Y. T. Vu, J. E. Mark, L. H. Pham and M. Engelhardt, *J. Appl. Polym. Sci.*, 2001, **82**, 1391.
18 M. A. Priolo, D. Gamboa, K. M. Holder and J. C. Grunlan, *Nano Lett.*, 2010, **10**, 4970.
19 Y. Kojima, A. Usuki, M. Kawasumi, Y. Fukushima, A. Okada, T. Kurauchi and O. Kamigaito, *J. Mater. Res.*, 1993, **8**, 1185.
20 D. L. Ho, R. M. Briber and C. J. Glinka, *Chem. Mater.*, 2001, **13**, 1923.
21 C. M. Roland, S. Hensel-Bielowka, M. Paluch and R. Casalini, *Rep. Prog. Phys.*, 2005, **68**, 1405.
22 C. M. Roland and R. Casalini, *J. Chem. Phys.*, 2005, **122**, 134505.
23 M. Mehrabzadeh and M. R. Kamal, *Polym. Eng. Sci.*, 2004, **44**, 152.
24 T. Pinnavaia and G. Beall, *Polymer-Clay Nanocomposites*, 2000, Wiley, New York.
25 E. Guth, *J. Appl. Phys.*, 1945, **16**, 20.
26 R. B. Bogoslovov, C. M. Roland, A. R. Ellis, A. M. Randall and C. G. Robertson, *Macromolecules*, 2008, **41**, 1289.
27 C. G. Robertson and X. Wang, *Phys. Rev. Lett.*, 2005, **95**, 075703.
28 J. A. C. Harwood and A. R. Payne, *J. Appl. Polym. Sci.*, 1966, **10**, 315.
29 G. Kraus, K. W. Rollmann and J. T. Gruver, *Macromolecules*, 1970, **3**, 92.
30 C. M. Roland, *Viscoelastic Behavior of Rubbery Materials*, Oxford, 2011.
31 R. Khrisnamoorti, J. Ren and A. S. Silvan, *J. Chem. Phys.*, 2001, **114**, 4958.
32 T. Wan, M. J. Clifford, F. Gao, A. S. Bailey, D. H. Gregory and R. Somsunan, *Polymer*, 2005, **46**, 6429.
33 A. Durmus, A. Kasgoz and C. W. Macosko, *Polymer*, 2007, **48**, 4492.
34 *Broadband Dielectric Spectroscopy*, ed. F. Kremer and A. Schonhals, Springer, Berlin, 2003.
35 P. A. M. Steeman and J. van Turnhout, in *Broadband Dielectric Spectroscopy*, ed. F. Kremer and A. Schonhals, Springer, 2003.
36 U. Buchenau, M. Ohl and A. Wischnewski, *J. Chem. Phys.*, 2006, **124**, 094505.
37 R. Casalini and C. M. Roland, *J. Non-Cryst. Solids*, 2007, **353**, 3936.
38 W. G. Hoover and M. Ross, *Contemp. Phys.*, 1971, **12**, 339.
39 Y. Hiwatari, H. Matsuda, T. Ogawa, N. Ogita and A. Ueda, *Prog. Theor. Phys.*, 1974, **52**, 1105.
40 C. M. Roland, S. Bair and R. Casalini, *J. Chem. Phys.*, 2006, **125**, 124508.
41 D. Coslovich and C. M. Roland, *J. Phys. Chem. B*, 2008, **112**, 1329.
42 N. P. Bailey, U. R. Pedersen, N. Gnan, T. B. Schroder and J. C. Dyre, *J. Chem. Phys.*, 2008, **129**, 184508.
43 C. M. Roland, R. Casalini, R. Bergman and J. Mattsson, *Phys. Rev. B: Condens. Matter Mater. Phys.*, 2008, **77**, 012201.

SUPPLEMENTARY MATERIAL

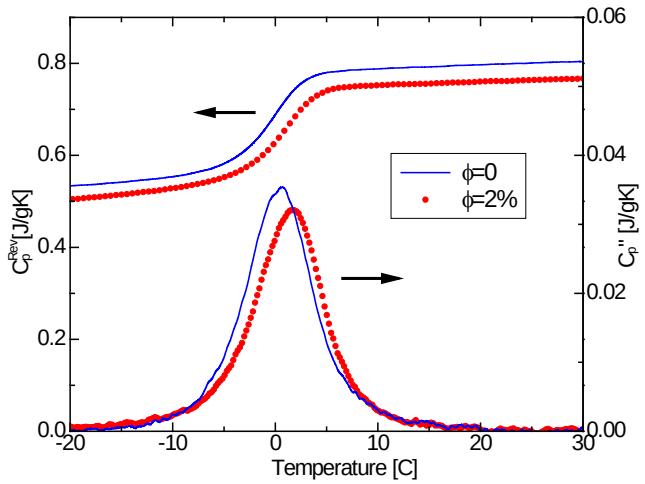

Figure. Reversible and imaginary components of MDSC for PCB with ϕ=0 (line) and 1.8% nanoclay (circles).

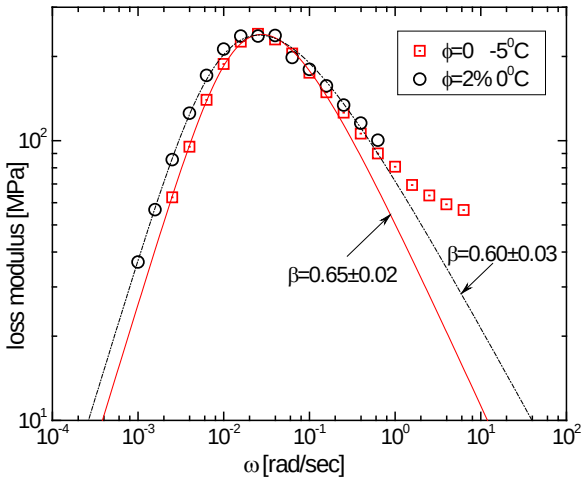

Figure. Dynamic shear modulus for the PCB neat (squares) and with 2% nanoclay (circles). The ordinate values for the composite were shifted to coincide with the neat PCB at the peak maximum.

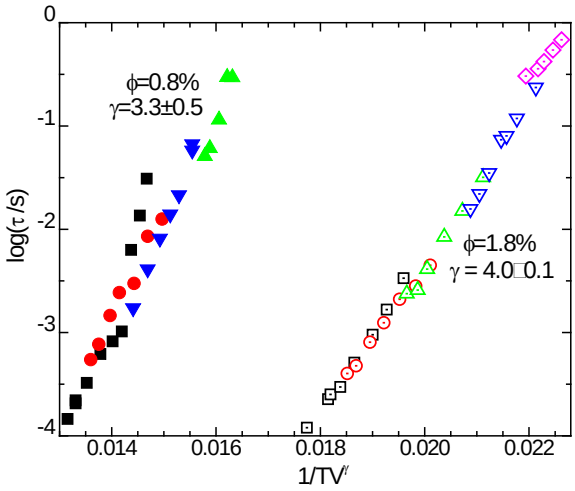

Figure. Scaling plots of the α' peak in the dielectric spectra of PCB ϕ=0.8 (filled symbols) and 1.8% (dotted open symbols). The quality of the scaling is inferior to that of the primary α relaxation, and the exponent is smaller, reflecting the weaker pressure dependence.